THE JOURNAL OF BIOLOGICAL CHEMISTRY VOL. 287, NO. 19, pp. 15466–15478, May 4, 2012

Endocannabinoids Stimulate Human Melanogenesis via Type-1 Cannabinoid Receptor*

Received for publication, October 18, 2011, and in revised form, March 1, 2012 Published, JBC Papers in Press, March 19, 2012, DOI 10.1074/jbc.M111.314880

Mariangela Pucci[‡1], Nicoletta Pasquariello[‡1], Natalia Battista[‡§1], Monia Di Tommaso[‡], Cinzia Rapino[‡], Filomena Fezza[§¶], Michela Zuccolo[‖], Roland Jourdain[‖], Alessandro Finazzi Agrò[¶], Lionel Breton[‖], and Mauro Maccarrone[‡§2]**

*From the [‡]Department of Biomedical Sciences, University of Teramo, 64100 Teramo, Italy, [‖]L'Oréal Research and Innovation, 92110 Clichy, France, [¶]Department of Experimental Medicine and Biochemical Sciences, University of Rome, "Tor Vergata," 00133 Rome, Italy, **Center for Integrated Research (CIR), University Campus Biomedico di Roma, 00128 Rome, Italy, and [§]European Center for Brain Research (CERC), Santa Lucia Foundation, 00143 Rome, Italy*

Background: Endocannabinoids like anandamide (AEA) play a key role in skin biology.
Results: At high concentrations, AEA induces apoptosis of primary human melanocytes through TRPV1 receptors, whereas at low concentrations, it stimulates melanogenesis through CB_1 receptors.
Conclusion: AEA regulates cell death or melanin synthesis through different pathways.
Significance: The double effect of AEA on human melanocytes might have implications beyond skin biology.

We show that a fully functional endocannabinoid system is present in primary human melanocytes (normal human epidermal melanocyte cells), including anandamide (AEA), 2-arachidonoylglycerol, the respective target receptors (CB_1, CB_2, and TRPV1), and their metabolic enzymes. We also show that at higher concentrations AEA induces normal human epidermal melanocyte apoptosis (~3-fold over controls at 5 μM) through a TRPV1-mediated pathway that increases DNA fragmentation and p53 expression. However, at lower concentrations, AEA and other CB_1-binding endocannabinoids dose-dependently stimulate melanin synthesis and enhance tyrosinase gene expression and activity (~3- and ~2-fold over controls at 1 μM). This CB_1-dependent activity was fully abolished by the selective CB_1 antagonist SR141716 or by RNA interference of the receptor. CB_1 signaling engaged p38 and p42/44 mitogen-activated protein kinases, which in turn activated the cyclic AMP response element-binding protein and the microphthalmia-associated transcription factor. Silencing of tyrosinase or microphthalmia-associated transcription factor further demonstrated the involvement of these proteins in AEA-induced melanogenesis. In addition, CB_1 activation did not engage the key regulator of skin pigmentation, cyclic AMP, showing a major difference compared with the regulation of melanogenesis by α-melanocyte-stimulating hormone through melanocortin 1 receptor.

Endocannabinoids (eCBs)[3] are endogenous fatty acid amides and monoacylglycerols whose prototypical members are *N*-arachidonoylethanolamine (anandamide (AEA)), and 2-arachidonoylglycerol (2-AG) (1). eCBs bind to type-1 (CB_1) and type-2 (CB_2) G protein-coupled cannabinoid receptors (2, 3). In addition, AEA at variance with 2-AG also binds to transient receptor potential vanilloid-1 (TRPV1) channels, which are activated by capsaicin, the pungent ingredient of hot chili pepper, and by noxious stimuli like heat and protons (4). The biological activity of eCBs at their receptors is generally subjected to a metabolic control mainly based on (i) Ca^{2+}-dependent biosynthesis catalyzed by *N*-acylphosphatidylethanolamine-specific phospholipase D (NAPE-PLD) for AEA (5) and by a specific phospholipase C that generates diacylglycerol (DAG), which is then converted to 2-AG by an *sn*-1-DAG lipase (DAGL), for 2-AG (6) and (ii) intracellular AEA degradation by fatty acid amide hydrolase (FAAH) (7) and by a specific monoacylglycerol lipase (MAGL) for 2-AG (8). Altogether, eCBs, their target receptors, and metabolic enzymes form the so-called "endocannabinoid system (ECS)" (9). In addition to the above listed elements, new components are being discovered as *bona fide* members of the ECS, including novel biosynthetic or degrading enzymes (10), novel receptorial targets (11, 12), and proteins responsible for transport and intracellular trafficking of eCBs (9).

* This work was supported by L'Oréal Research and Innovation, Paris and by Fondazione Cassa di Risparmio di Teramo Grant 2009-2012 (to M. M.).
[1] These authors contributed equally to this work.
[2] To whom correspondence should be addressed: Dept. of Biomedical Sciences, University of Teramo, Piazza A. Moro 45, Teramo, 64100 Italy. Tel.: 39-0861-266875; Fax: 39-0861-266877; E-mail: mmaccarrone@unite.it.
[3] The abbreviations used are: eCB, endocannabinoid; ACEA, arachidonoyl-2′-chloroethylamide; AEA, *N*-arachidonoylethanolamine; 2-AG, 2-arachidonoylglycerol; CB_1, type-1 G protein-coupled cannabinoid receptor; CB_2, type-2 G protein-coupled cannabinoid receptor; CPS, capsaicin; CREB, cyclic AMP response element-binding protein; DAG, diacylglycerol; DAGL, *sn*-1-DAG lipase; ECS, endocannabinoid system; FAAH, fatty acid amide hydrolase; H89, *N*-[2-(*p*-bromocinnamylamino)ethyl]-5-isoquinoline sulfonamide; I-RTX, 5′-iodoresiniferatoxin; mAEA, *R*(+)-methanandamide; MAGL, monoacylglycerol lipase; MC1R, melanocortin 1 receptor; MITF, microphthalmia-associated transcription factor; α-MSH, α-melanocyte-stimulating hormone; NAPE-PLD, *N*-acylphosphatidylethanolamine-specific phospholipase D; pCREB, phospho-CREB; RTX, resiniferatoxin; SR141716, *N*-piperidino-5-(4-chlorophenyl)-1-(2,4-dichlorophenyl)-4-methyl-3-pyrazolecarboxamide; SR144528, *N*-[(1*S*)-*endo*-1,3,3-trimethyl-1-bicyclo[2.2.1]heptan-2-yl]5-(4-choro-3-methylphenyl)-1-(4-methylbenzyl)pyrazole-3-carboxamide; TRPV1, transient receptor potential vanilloid-1; TYR, tyrosinase; CP55.940, 5-(1,1-dimethylheptyl)-2-[5-hydroxy-2-(3-hydroxypropyl)cyclohexyl]phenol; PD98059, 2-(2-amino-3-methoxyphenyl)-4*H*-1-benzopyran-4-one; SB203580, 4-(4-fluorophenyl)-2-(4-methylsulfinylphenyl)-5-(4-pyridyl)-1*H*-imidazole; JWH133, (6a*R*,10a*R*)-3-(1,1-dimethylbutyl)-6a,7,10,10a-tetrahydro-6,6,9-trimethyl-6*H*-dibenzo[*b*,*d*]pyran; NHEM, normal human epidermal melanocyte; qRT-PCR, quantitative real time RT-PCR.

To date, many biological activities of ECS have been documented both within the central nervous system and in the periphery (9, 13). In particular, growing evidence suggests a key role for eCB signaling in skin biology (14–16) with a potential future exploitation for therapies in dermatology (17, 18). In fact, eCBs have been shown to inhibit terminal differentiation (cornification) of human keratinocytes through CB_1 receptors (19). The latter receptors inhibited hair shaft elongation and the proliferation of hair matrix keratinocytes in the hair follicle (20). On the other hand, CB_2 receptors might act as cutaneous nociceptors (21, 22), whereas in human sebocytes, they up-regulate the expression of key genes involved in lipid synthesis in a paracrine/autocrine manner (23). Furthermore, a protective role of ECS has been reported in contact allergy of the skin (24).

Despite significant research on the role of eCB signaling in keratinocytes, no data are yet available on the presence and potential role of ECS in primary human melanocytes. Previous studies have shown the mRNA and protein expression of CB_1 and CB_2 in melanoma cell lines of murine and human origin (25, 26) and of CB_1 in nontumorigenic, immortalized melanocytic cell lines (25). In addition, endogenous expression of TRPV1 channels has been documented in cultured human melanocytes (27). Primary human melanocytes, which are a truly physiological model, are derived from the neural crest cells (28) and are responsible for skin pigmentation (melanogenesis). In the basal layer of the skin, which separates dermis and epidermis, each melanocyte is surrounded by ~35 keratinocytes, forming the so-called "epidermal melanin unit" (29). This tight association allows the transport of melanin from melanocytes to the overlaying keratinocytes, *e.g.* upon exposure of the latter cells to solar ultraviolet (UV) radiation (30, 31). In fact, melanin production mediated by the enzyme tyrosinase (32) and delivery to keratinocytes is the main skin photoprotective mechanism as it prevents UV-induced DNA damage in the epidermis (30, 31). Here we sought to ascertain whether primary human melanocytes (normal human epidermal melanocyte (NHEM) cells) have the components of the ECS by analyzing them at the mRNA, protein, and functional level. Then we investigated the possible modulation of NHEM cell survival and death and of melanin synthesis by eCBs. In this context, we checked the effect of eCBs on the expression of the microphthalmia-associated transcription factor (MITF), a protein of the basic helix-loop-helix leucine zipper family, regarded as a master regulator of vertebrate melanogenesis (33).

EXPERIMENTAL PROCEDURES

Materials and Antibodies—AEA (*N*-arachidonoylethanolamine), 5-(1,1-dimethylheptyl)-2-[5-hydroxy-2-(3-hydroxypropyl)cyclohexyl]phenol (CP55.940), *R*(+)-arachidonyl-1′-hydroxy-2′-propylamide (*R*(+)-methanandamide (mAEA)), 8-methyl-*N*-vanillyl-*trans*-6-nonenamide (capsaicin (CPS)), forskolin, *N*-[2-(*p*-bromocinnamylamino)ethyl]-5-isoquinoline sulfonamide (H89), 3,4-dihydroxy-L-phenylalanine, and α-melanocyte-stimulating hormone (α-MSH) were purchased from Sigma. Arachidonoyl-2′-chloroethylamide (ACEA) was from Cayman Chemical (Ann Arbor, MI). 2-(2-Amino-3-methoxyphenyl)-4*H*-1-benzopyran-4-one (PD98059) and 4-(4-fluorophenyl)-2-(4-methylsulfinylphenyl)-5-(4-pyridyl)-1*H*-imidazole (SB203580) were from Calbiochem. 2-AG and resiniferatoxin (RTX) were purchased from Alexis Corp. (San Diego, CA). *N*-Piperidino-5-(4-chlorophenyl)-1-(2,4-dichlorophenyl)-4-methyl-3-pyrazolecarboxamide (SR141716) and *N*-[(1*S*)-*endo*-1,3,3-trimethyl-1-bicyclo[2.2.1]heptan-2-yl]5-(4-choro-3-methylphenyl)-1-(4-methylbenzyl)pyrazole-3-carboxamide (SR144528) were kind gifts from Sanofi-Aventis Recherche (Montpellier, France). (6a*R*,10a*R*)-3-(1,1-Dimethylbutyl)-6a,7,10,10a-tetrahydro-6,6,9-trimethyl-6*H*-dibenzo[*b*,*d*]pyran (JWH133) and 5′-iodoresiniferatoxin (I-RTX) were from Tocris-Cookson (Bristol, UK). *N*-[^{3}H]Arachidonoylphosphatidylethanolamine (200 Ci/mmol) and 2-[^{3}H]oleoylglycerol (20 Ci/mmol) were purchased from American Radiolabeled Chemicals, Inc. (St. Louis, MO). [^{3}H]AEA (205 Ci/mmol), [^{3}H]CP55.940 (126 Ci/mmol), and [^{3}H]RTX (43 mCi/mmol) were from Perkin-Elmer Life Sciences. 1-[^{14}C]Stearoyl-2-arachidonoyl-*sn*-glycerol (56 mCi/mmol) was from Amersham Biosciences. Human recombinant Agouti-related signaling protein was from Creative BioMart (Shirley, NY). d_8-AEA and d_8-2-AG were from Cayman Chemical Co.

Rabbit anti-β-actin polyclonal antibody was purchased from Cell Signaling Technology (Danvers, MA). Rabbit anti-tyrosinase and anti-MITF polyclonal antibodies were from Abcam (Cambridge, UK). Rabbit anti-CB_1, anti-CB_2, anti-NAPE-PLD, and anti-MAGL polyclonal antibodies were from Cayman Chemical Co. Rabbit anti-DAGL and anti-TRPV1 polyclonal antibodies and goat anti-rabbit antibodies conjugated to horseradish peroxidase (HRP) were purchased from Santa Cruz Biotechnology (Santa Cruz, CA). Goat anti-rabbit antibodies conjugated to alkaline phosphatase were from Bio-Rad.

Cell Culture and Treatment and Determination of Apoptosis—Primary human melanocytes (NHEMs) from foreskin (Promocell, Heidelberg, Germany) were grown for 24 h at 37 °C in a humidified 5% CO_2 atmosphere in M2 melanocyte growth medium (Promocell) according to the manufacturer's instructions. AEA and related substances were added directly to culture medium, and vehicles alone were added to controls. Twenty-four hours after each treatment, cell viability was measured by trypan blue dye exclusion as reported (19).

Apoptotic cell death was quantified after 24 h of treatment by ELISA based on the evaluation of DNA fragmentation through an immunoassay for histone-associated DNA fragments in the cell cytoplasm (Roche Diagnostics). Specific determination of mono- and oligonucleosomes in the cytoplasmic fraction of cell lysates was performed by measuring the absorbance values at 405 nm as reported (34). Apoptosis was also quantified by measuring mRNA expression of p53, a typical marker of programmed cell death (35), by quantitative real time reverse transcription-polymerase chain reaction (qRT-PCR) (see below).

qRT-PCR Analysis—RNA was extracted from NHEM cells using the RNeasy extraction kit (Qiagen, Crawley, UK) as suggested by the manufacturer. qRT-PCR assays were performed using the SuperScript III Platinum Two-Step qRT-PCR kit (Invitrogen). One microgram of total RNA was used to produce cDNA with 10 units/μl SuperScript III reverse transcriptase in the presence of 2 units/μl RNaseOUT, 1.25 μM oligo(dT)$_{20}$, 1.25 ng/μl random hexamers, 5 mM $MgCl_2$, 0.5 mM dNTP mixture, and diethyl pyrocarbonate-treated water. The reaction was

performed using the following qRT-PCR program: 25 °C for 10 min, 42 °C for 50 min, and 85 °C for 5 min; then after addition of 0.1 unit/μl *Escherichia coli* RNase H, the product was incubated at 37 °C for 20 min. The target transcripts were amplified using an ABI PRISM 7700 sequence detector system (Applied Biosystems, Foster City, CA). Human primers for CB_1, CB_2, TRPV1, NAPE-PLD, FAAH, DAGL, MAGL, p53, and β-actin were as reported (35). In addition, the following primers were used: human TYR F, 5′-ATGACCTCTTTGTCTGGATGC-3′; human TYR R, 5′-AAGAGGAGAAGAATGATGC-3′; human MITF F, 5′-ATGACATCACGCATCTT GC-3′; human MITF R, 5′-TACTGCTTTACC TGCTGC-3′. β-Actin was used as a housekeeping gene for quantification.

One microliter of the first strand of cDNA product was used (in triplicate) for amplification in 25 μl of reaction solution containing 12.5 μl of Platinum SYBR Green qPCR SuperMix-UDG (Invitrogen) and 10 pmol of each primer. The following PCR program was used: 95 °C for 10 min and 40 amplification cycles at 95 °C for 30 s, 56 °C for 30 s, and 72 °C for 30 s.

Immunochemical Analysis—Cells were lysed in ice-cold lysis buffer (10 mM EDTA, 50 mM Tris-HCl (pH 7.4), 150 mM sodium chloride, 1% Triton X-100, 2 mM phenylmethylsulfonyl fluoride, 2 mM sodium orthovanadate, 10 mg/ml leupeptin, 2 mg/ml aprotinin), and protein content was determined by the Bio-Rad Protein Assay kit. For Western blotting, equal amounts of protein (25 μg/lane) were loaded onto 10% sodium dodecyl sulfate-polyacrylamide gels and electroblotted onto polyvinylidene fluoride sheets (Amersham Biosciences). Membranes were blocked with 10% nonfat dried milk and 5% bovine serum albumin for 2 h and then incubated with anti-CB_1 (1:100), anti-CB_2 (1:200), anti-TRPV1 (1:200), anti-NAPE-PLD (1:100), anti-FAAH (1:500), anti-DAGL (1:1000), anti-MAGL (1:200), anti-MITF (1:200), anti-TYR (1:100), or anti-β-actin (1:100) antibodies. Then membranes were rinsed and incubated with HRP-conjugated secondary antibody (diluted 1:2000) in blocking solution. Detection of the immunoreactive bands was performed in a West Dura Chemiluminescence System (Pierce) using as positive controls homogenates (25 μg of protein/well) of mouse brain (for CB_1, NAPE-PLD, FAAH, DAGL, and MAGL), mouse spleen (for CB_2), or human HeLa cells (for TRPV1) as reported (36). For ELISA tests, NHEM homogenates (20 μg of protein/well) were incubated with anti-TYR antibodies (1:1000) and then with goat anti-rabbit secondary antibody (diluted 1:2000) conjugated to alkaline phosphatase (34). Tyrosinase protein levels were expressed as -fold increase over vehicle-treated controls that showed absorbance values at 405 nm of 0.220 ± 0.025.

Functional Assays of ECS and Metabolism of AEA—The synthesis of [^{3}H]AEA by NAPE-PLD (phospholipase D) was assayed in NHEM cell homogenates (100 μg of protein/test) using 100 μM *N*-[^{3}H]arachidonoylphosphatidylethanolamine and reversed phase high performance liquid chromatography (HPLC) as reported (37). The hydrolysis of [^{3}H]AEA (10 μM) by FAAH (amidase) was assayed in NHEM cell extracts (50 μg of protein/test) by measuring the release of [^{3}H]ethanolamine as reported (38). Both NAPE-PLD and FAAH activities were expressed as pmol of product released/min/mg of protein.

Metabolism of 2-AG—To evaluate the synthesis of 2-[^{14}C]AG by DAGL, NHEM cell homogenates (200 μg protein/test) were incubated at 37 °C for 30 min with 500 μM 1-[^{14}C]stearoyl-2-arachidonoyl-*sn*-glycerol as reported (39). Then a mixture of chloroform/methanol (2:1, v/v) was added to stop the reaction, and the organic phase was dried and fractionated by TLC on silica using polypropylene plates with chloroform/methanol/NH_4OH (94:6:0.3, v/v/v) as eluent. The release of 2-[^{14}C]AG was measured by cutting the corresponding TLC spots followed by scintillation counting. The hydrolysis of 2-[^{3}H]AG by MAGL was assayed in NHEM cell supernatants (100 μg of protein/test) obtained at 39,000 × *g* and incubated with 10 μM 2-[^{3}H]oleoylglycerol at 37 °C for 30 min (40). The reaction was stopped with a mixture of chloroform/methanol (2:1, v/v), and the release of [^{3}H]glycerol in the aqueous phase was measured in a β-counter (PerkinElmer Life Sciences). Both DAGL and MAGL activities were expressed as pmol of product/min/mg of protein.

CB and TRPV1 Receptor Binding—For cannabinoid receptor studies, NHEM cells were resuspended in 2 mM Tris-EDTA, 320 mM sucrose, 5 mM $MgCl_2$ (pH 7.4), and then they were homogenized in a Potter homogenizer and centrifuged as reported (36). The resulting pellet was resuspended in assay buffer (50 mM Tris-HCl, 2 mM Tris-EDTA, 3 mM $MgCl_2$, 1 mM PMSF, pH 7.4) to a protein concentration of 1 mg/ml. The membrane preparation was divided into aliquots, which were stored at −80 °C for no longer than 1 week. These membrane fractions (100 μg of protein/test) were used in rapid filtration assays with the synthetic cannabinoid [^{3}H]CP55.940 (400 pM) as described (36). The binding of the TRPV1 agonist [^{3}H]RTX (500 pM) was also evaluated by rapid filtration assays (36). Unspecific binding was determined in the presence of cold agonists (1 μM CP55.940 or 1 μM RTX) and further validated by selective antagonists (0.1 μM SR141716 for CB_1, 0.1 μM SR144528 for CB_2, and 1 μM I-RTX for TRPV1) as reported (36).

Endogenous Levels of Endocannabinoids—The lipid fraction from NHEM cells was extracted with chloroform/methanol (2:1, v/v) in the presence of d_8-AEA and d_8-2-AG as internal standards. The organic phase was dried and then analyzed by liquid chromatography-electrospray ionization mass spectrometry using a single quadrupole API-150EX mass spectrometer (Applied Biosystems) in conjunction with a PerkinElmer LC system (PerkinElmer Life Sciences). Quantitative analysis was performed by selected ion recording over the respective sodiated molecular ions as reported (36).

Determination of Melanin Content—Melanin content in NHEM cells was determined as reported previously (41). Briefly, NHEM cells were treated with AEA and related compounds for 24 h, washed, placed in M2 melanocyte growth medium for a further 48 h, then harvested by trypsin, and washed twice with phosphate-buffered saline. The samples were resuspended in 200 μl of Milli-Q water, and 1 ml of ethanol/ether mixture (1:1, v/v) was added to remove opaque substances other than melanin. After 15 min, samples were centrifuged at 600 × *g* for 5 min, and the precipitate was air-dried and dissolved in 200 μl of 1 N NaOH. Samples were then heated at 80 °C for 1 h and cooled down, and the amount of melanin was

determined spectrophotometrically at 450 nm using melanin standards (Sigma) to ascertain the linearity range of the assay. Melanin content was expressed as -fold increase over vehicle-treated controls, which contained 90 ± 10 μg of melanin/mg of protein.

Assay of Tyrosinase Activity—Tyrosinase activity was determined as reported previously (41). Briefly, NHEM cells were solubilized in 1 ml of phosphate-buffered saline containing 0.5% Triton X-100 and 10 μl of protease inhibitor mixture (Sigma). After sonication for 20 s on ice, the extracts were clarified by centrifugation at 25,000 × *g* for 15 min at 4 °C, and aliquots (30 μg of protein) were incubated for 1 h at 37 °C with 0.05% 3,4-dihydroxy-L-phenylalanine in 0.1 M sodium phosphate buffer (pH 7.0) in a final volume of 200 μl. Dopachrome formation from 3,4-dihydroxy-L-phenylalanine was measured at 490 nm using an iMark microplate reader (Bio-Rad). The absorbance values of the samples were within the linearity range of a standard curve obtained with purified mushroom tyrosinase (Sigma). Tyrosinase activity was expressed as -fold increase over vehicle-treated controls, which contained 0.037 ± 0.005 unit/μg of protein.

RNA Interference—Synthetic ready to use small (21-nucleotide) interfering RNA (siRNA) complementary to a region of CB_1, TYR, and MITF and non-silencing control siRNAs were custom-synthesized by Qiagen (Tokyo, Japan). NHEM cells were transfected with 600 pmol of siRNA using Lipofectamine 2000 reagent as reported (35). Briefly, 600 pmol of siRNA and 30 μl of Lipofectamine 2000 were diluted with Opti-MEM to a final volume of 3 ml, mixed, and added to NHEM cells grown to 60% confluence in 100-mm-diameter plates. After 6 h, cells were washed and then cultured in fresh medium for 24 h. Cells were then washed and cultured for 24 h in medium containing mAEA (1 μM), and finally qRT-PCR analysis and Western blotting were performed.

Determination of cAMP Content—Intracellular cAMP content was measured by the Cyclic AMP Enzyme Immunoassay kit (Cayman Chemical Co.) according to the manufacturer's instructions. Briefly, NHEM cells were treated with 1 μM AEA or 100 nM α-MSH for 24 h, and then the cells were plated in 6-well dishes at a density of 5×10^4 cells/well and lysed in 0.1 M HCl (230 μl) for 20 min at room temperature. Lysates were centrifuged at 1000 × *g* for 10 min at 4 °C, and the supernatants were used to quantify cAMP content. As a positive control, NHEM cells were also treated for 24 h with the cAMP activator forskolin (20 μM) as reported (42).

Assay of Phospho-CREB Content—The CREB (Phospho-Ser133) Transcription Factor Assay kit (Cayman Chemical Co.) was used according to the manufacturer's instructions. This kit measures the amount of phospho-CREB (pCREB) bound to an oligonucleotide containing the cyclic AMP response element sequence (TGACGTCA) by means of specific anti-pCREB antibodies. Briefly, nuclear proteins were extracted from NHEM cells (43) that had been treated for 24 h with 1 μM mAEA and related compounds. NHEM cells were also treated with 1 μM mAEA in the presence of the protein kinase A (PKA) inhibitor H89 (5 μM) or with 100 nM α-MSH alone or in the presence of 5 μM H89 as described (42). Aliquots of nuclear proteins (10 μg/well) were then incubated overnight in 96-well plates as suggested by the manufacturer.

TABLE 1
Endocannabinoids and their metabolic enzymes and receptors in human NHEM cells

ECS component	Activity/amount
AEA[a]	0.11 ± 0.01
2-AG[a]	74 ± 5
NAPE-PLD[b]	108 ± 2
FAAH[b]	78 ± 8
DAGL[b]	393 ± 12
MAGL[b]	874 ± 7
CB[c]	71 ± 5
CB[c] + SR141716 (0.1 μM)	42 ± 3
CB[c] + SR144528 (0.1 μM)	28 ± 2
TRPV1[c]	200 ± 10
TRPV1[c] + I-RTX (1 μM)	32 ± 2

[a] Content (pmol/mg of protein).
[b] Activity (pmol/min/mg of protein).
[c] Binding (fmol/mg of protein).

TABLE 2
Comparison of qRT-PCR standard curves of ECS elements in human NHEM cells

Gene	Slope	r^2	C_t	Copy numbers[a]	mRNA copies[b]
CB_1	−1.546	0.996	32.83 ± 0.27	13 ± 0.11	3.58*e*−06
CB_2	−1.196	0.973	28.41 ± 0.03	16 ± 0.02	4.36*e*−06
TRPV1	−1.546	0.996	21.99 ± 0.16	14280 ± 103.9	3.98*e*−03
NAPE-PLD	−1.412	0.976	20.28 ± 0.04	5817 ± 11.47	1.62*e*−03
FAAH	−1.374	0.999	23.27 ± 0.23	1122 ± 11.09	3.13*e*−04
MAGL	−1.444	0.960	19.04 ± 0.03	11648 ± 18.35	3.24*e*−03
DAGL	−1.651	0.976	26.98 ± 0.19	456 ± 3.21	1.27*e*−04

[a] Values are per 50 ng of cDNA.
[b] Data were normalized to gene copies of the housekeeping gene β-actin.

Statistical Analysis—Data reported in this study are the means ± S.E. of at least three independent experiments, each performed in triplicate. Data were compared by one-way analysis of variance followed by Bonferroni's post hoc test using the GraphPad Prism4 program (GraphPad Software for Science, San Diego, CA).

RESULTS

ECS in NHEM Cells—The presence of the main endocannabinoids, AEA and 2-AG, could be detected in primary human melanocytes (NHEM cells) through LC-MS analysis (Table 1). Consistently, these cells were found to express at transcriptional, translational, and functional levels all the ECS elements that bind and metabolize AEA or 2-AG. First of all, qRT-PCR analysis demonstrated mRNA transcripts for the main elements of ECS, including CB_1, CB_2, TRPV1, NAPE-PLD, FAAH, DAGL, and MAGL. In particular, TRPV1 and MAGL transcripts were the most abundant followed by NAPE-PLD, FAAH, and DAGL, whereas both cannabinoid receptors were the least expressed (Table 2). Next, translation of ECS mRNAs into the corresponding proteins was checked by Western blotting, which showed that all ECS elements detected as mRNAs were also present at the protein level (Fig. 1). Furthermore, the activity of the ECS elements was tested by biochemical assays, which demonstrated that all the enzymes and receptors detected in NHEM cells were functional (Table 1). In keeping with the mRNA expression data, it was found that TRPV1 binding capacity was higher than that of CB receptors. The binding of the synthetic cannabinoid [^{3}H]CP55.940, a CB_1 and CB_2 agonist (3), was reduced to ~60% of the controls by 0.1 μM

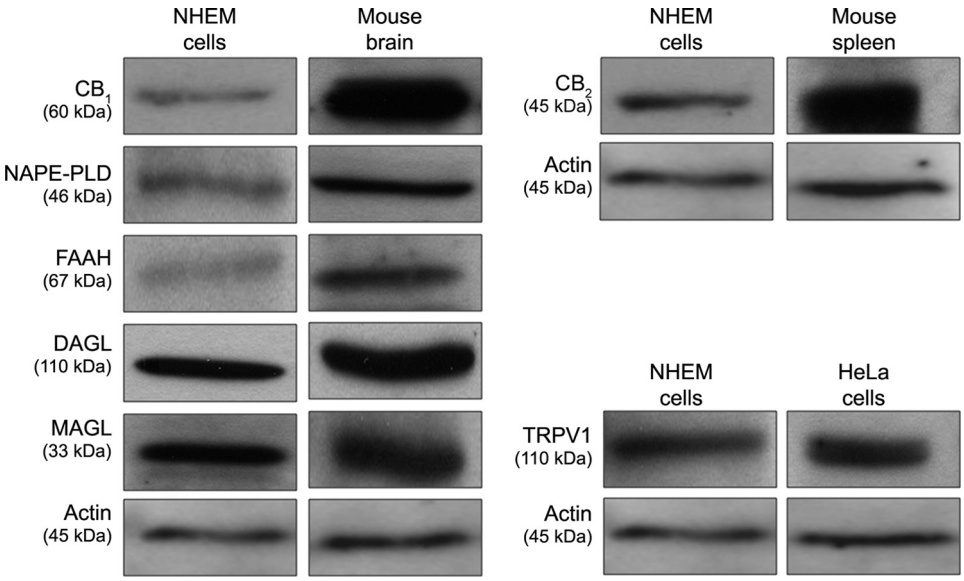

FIGURE 1. **Characterization of ECS in primary human melanocytes.** The Western blot analysis of the major ECS elements in NHEM cells included homogenates of mouse brain, mouse spleen, and human HeLa cells as positive controls.

SR141716, a selective CB_1 antagonist (3), and to ~40% by 0.1 μM SR144528, a selective CB_2 antagonist (3). These data indicate that both CB subtypes were functional to a similar extent in human NHEM cells (Table 1). However, some discrepancies were observed between the activity and mRNA expression of AEA- and 2-AG-metabolizing enzymes, a finding that is not unprecedented for ECS elements (35, 44). Overall, the present data demonstrate that primary human melanocytes have a complete and fully functional ECS.

Induction of Apoptosis—AEA at micromolar concentrations has been shown to trigger apoptosis in different cell types (34, 44, 45). Here we treated NHEM cells for 24 h with different amounts of mAEA, a non-hydrolyzable analog that binds the same targets and with the same affinity as AEA (3) and shows the same functional effects as the natural compound (3, 4). mAEA was able to reduce cell viability dose-dependently (in the range of 0–25 μM), reaching statistical significance at concentrations ≥5 μM (Fig. 2*A*). At 5 μM, mAEA reduced NHEM viability to ~65% of controls (Fig. 2*A*). To ascertain whether the observed cytotoxicity was indeed due to programmed cell death, DNA fragmentation, a hallmark of apoptosis (Ref. 34 and references therein), was measured. mAEA dose-dependently induced NHEM cell apoptosis as shown by ELISA tests with a ~3-fold increase in DNA fragmentation over controls at 5 μM mAEA (Fig. 2*B*). The same induction of apoptosis was observed by qRT-PCR evaluation of p53 mRNA expression (Fig. 2*B*), a typical marker of programmed cell death (Ref. 35 and references therein). Thus, p53 levels were checked to investigate the mechanism of cell death induced by mAEA, showing that either AEA or capsaicin, a selective agonist of TRPV1 receptors (4), at 5 μM concentration significantly enhanced p53 mRNA, whereas ACEA, a selective CB_1 agonist (3), JWH133, a selective CB_2 agonist (3), or 2-AG, which activates both CB_1 and CB_2 receptors but not TRPV1 (4), had no effect (Fig. 2*C*). Consistently, the effect of mAEA on p53 expression was fully prevented by 1 μM I-RTX, a selective TRPV1 antagonist (4), whereas the CB_1 and CB_2 selective antagonists SR141716 and SR144528 (3), both used at 0.1 μM, were ineffective (Fig. 2*C*). Every antagonist was used at concentrations previously shown to block the target receptor (35). Taken together, these data demonstrate that mAEA at concentrations ≥5 μM can induce NHEM cell apoptosis through TRPV1 receptors, thus extending to human melanocytes previous observations on many different cell types (for a review, see Ref. 46). In this context, it is noteworthy that cannabinoids have been shown to trigger apoptosis of melanoma cells but not of nontumorigenic melanocytic cell lines of murine or human origin (25). This observation and the present data underpin relevant differences between signaling pathways that direct cell survival and death in tumorigenic, nontumorigenic, and primary melanocytes, calling for caution when extrapolating data obtained with immortalized cells in culture to the *in vivo* situation. Then we tried to ascertain the possible role of non-toxic concentrations of mAEA on melanin synthesis, which is the most relevant biological activity of melanocytes in all vertebrates (29–31).

Induction of Melanogenesis—At low doses (0–3 μM; cell viability ≥85%; Fig. 2*A*), mAEA dose-dependently induced melanin production by NHEM cells (Fig. 3*A*). Melanin synthesis in NHEM cells exposed for 24 h to 1 μM mAEA was ~3-fold higher than in untreated controls. The increase of melanin content induced by 1 μM mAEA was also observed using AEA, ACEA, and 2-AG, whereas JWH133 and CPS at the same concentration (Fig. 3*B*) had no effect. Accordingly, SR141716 fully reverted the effect of mAEA, whereas SR144528 and I-RTX were ineffective (Fig. 3*B*). Therefore, these data demonstrate that melanin synthesis was increased by mAEA via a CB_1-dependent mechanism, which did not involve CB_2 or TRPV1. To further establish the role of CB_1 in human melanogenesis, the corresponding gene was ablated in NHEM cells by RNA interference. Silencing of CB_1 gene led to an almost complete disappearance of its mRNA and protein (Fig. 3*C*, *inset*) and abolished the effect of 1 μM mAEA on melanin production compared with controls (Fig. 3*C*). CB_1 receptors are known to trigger p38 and p42/44 mitogen-activated protein kinase (MAPK) activities

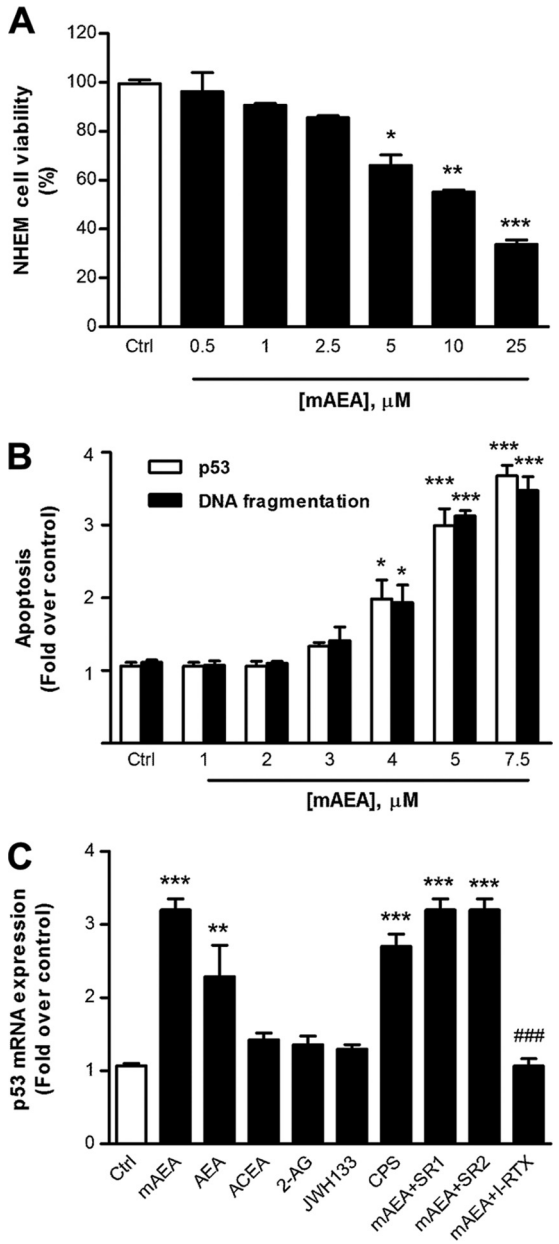

FIGURE 2. **Induction of NHEM cell apoptosis by mAEA and related compounds.** The effect of different doses of mAEA on cell viability (*A*) and apoptotic cell death (*B*) is shown. *C*, effect of mAEA, AEA, ACEA, 2-AG, JWH133, or CPS (each used at 5 μM) and of mAEA (5 μM) in combination with SR141716 (*SR1*; 0.1 μM), SR144528 (*SR2*; 0.1 μM), or I-RTX (1 μM) on p53 mRNA expression. SR141716, SR144528, and I-RTX were ineffective when used alone (not shown for the sake of clarity). *Error bars* represent S.E. values. *, $p < 0.05$; **, $p < 0.01$; ***, $p < 0.001$ *versus* control (*Ctrl*). ###, $p < 0.001$ *versus* mAEA.

(Ref. 35 and references therein). In fact, melanin production induced by 1 μM mAEA was dramatically decreased by 10 μM SB203580, a selective inhibitor of p38 MAPK, and by 10 μM PD98059, a selective inhibitor of p42/44 MAPK (Fig. 3*D*), at drug concentrations already shown to block the target enzymes (35).

Melanogenesis Induction by mAEA Requires Tyrosinase Activation—At the same dose (1 μM) that triples melanin production, mAEA also enhanced tyrosinase mRNA and protein expression (Fig. 4, *A* and *B*) as well as tyrosinase activity (Fig. 4*C*) by ~3- and ~2-fold, respectively. The effect on tyrosinase mRNA was reverted by 0.1 μM SR141716 but not by 0.1 μM SR144528 nor by 1 μM I-RTX (Fig. 4*A*). Consistent with these data, 1 μM CPS had no effect on tyrosinase mRNA expression (Fig. 4*A*), as a whole suggesting that the mAEA effect was dependent on CB_1 receptors only. Much like melanin synthesis, tyrosinase expression (Fig. 4, *A* and *B*) and activity (Fig. 4*C*) enhanced by mAEA through CB_1 was reduced by 10 μM SB203580 and by 10 μM PD98059, again suggesting that it involved p38 and p42/44 MAPK activities.

MITF Is Also Involved in mAEA-induced Melanogenesis—The mechanism of melanogenesis induction by mAEA was further investigated through RNA interference experiments. In particular, we silenced the gene encoding for tyrosinase and that encoding for MITF because it is known that MITF is the master upstream regulator of tyrosinase gene expression (31, 33, 47). RNA interference demonstrated that silencing tyrosinase or MITF gene reduced both tyrosinase mRNA (Fig. 5*A*) and protein levels (Fig. 5*A*, *inset*) and abolished the effect of mAEA on tyrosinase mRNA expression in NHEM cells (Fig. 5*A*). The tyrosinase silencing was ineffective on MITF mRNA and protein levels, whereas MITF silencing significantly reduced both (Fig. 5, *B* and *inset*). Furthermore, silencing tyrosinase did not abolish the effect of mAEA on MITF mRNA at variance with NHEM cells in which MITF was ablated (Fig. 5*B*). On the other hand, RNA interference of tyrosinase or MITF prevented the effect of mAEA on melanin content (Fig. 5*C*).

Comparison of Effect of mAEA on Melanogenesis with That of α-MSH—As expected, α-MSH, which is the physiological activator of melanogenesis (30, 31), at 100 nM was able to induce melanin synthesis (Fig. 6*A*) and tyrosinase gene expression (Fig. 6*B*). These effects were mediated by α-MSH binding to melanocortin 1 receptor (MC1R) as demonstrated by the ability of the selective MC1R antagonist Agouti-related signaling protein (10 nM) to prevent both (Fig. 6, *A* and *B*). Typically, MC1R activation increases cAMP, which activates PKA and CREB, which in turn up-regulates the expression of MITF and hence tyrosinase expression (42, 48, 49). It should be recalled that CREB is a ubiquitously expressed transcription factor, and its transcriptional activity is stimulated upon phosphorylation at Ser-133 by different protein kinases, including PKA, Ca^{2+}/calmodulin kinases II and IV, and several kinases in the MAPK cascade (50). Thus, CREB represents a site of convergence where diverse signaling pathways and their associated stimuli produce plasticity by altering gene expression (51).

In melanocytes, cAMP activates not only PKA but also p42/44 MAPK (52), which phosphorylates MITF, thus increasing its transcriptional activity (53, 54) and possibly regulating its stability and degradation (55). More recently, p38 MAPK signaling has been shown to be involved in α-MSH-induced MITF activation and tyrosinase transcription (56) as well as in melanogenesis triggered by natural products (57). In keeping with this background, MC1R was found to act through p38 and p42/44 MAPK activities because 10 μM SB203580 and 10 μM PD98059 completely prevented α-MSH-induced melanin synthesis (Fig. 6*A*) and tyrosinase mRNA production (Fig. 6*B*). Interestingly, the effects of α-MSH and mAEA on melanin synthesis and tyrosinase expression were partly (although not sig-

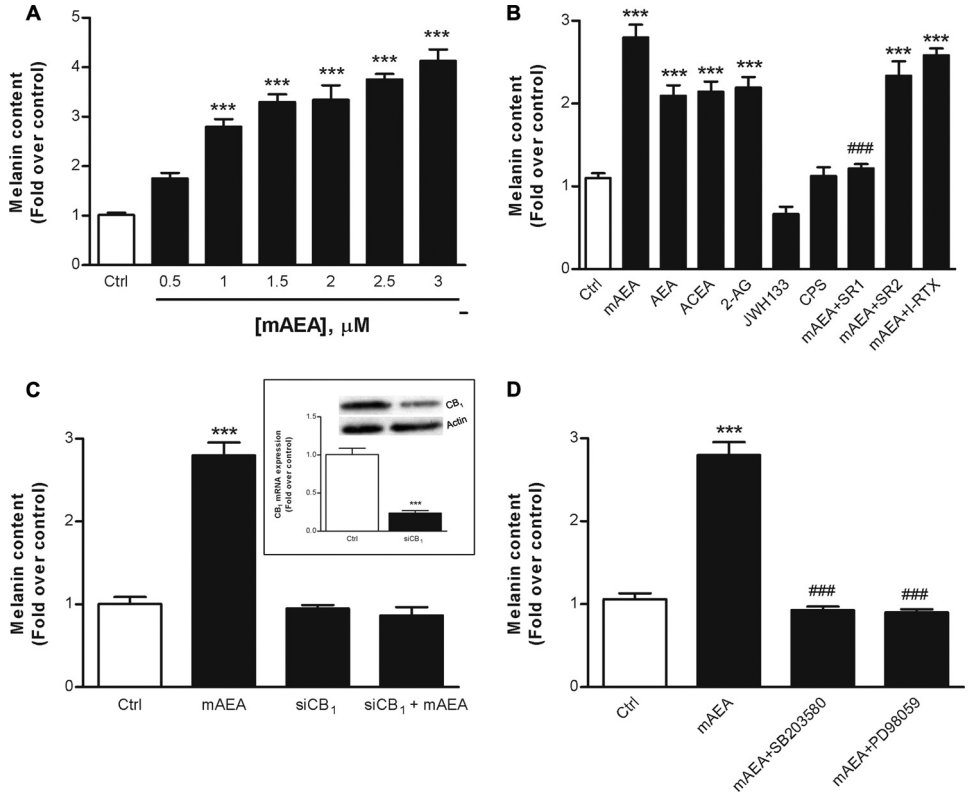

FIGURE 3. **Induction of melanogenesis by mAEA and related compounds.** *A*, effect of different non-toxic doses of mAEA on melanin synthesis. *B*, effect of mAEA, AEA, ACEA, 2-AG, JWH133, or CPS (each used at 1 μM) and of mAEA (1 μM) in combination with SR141716 (*SR1*; 0.1 μM), SR144528 (*SR2*; 0.1 μM) or I-RTX (1 μM). *C*, effect of CB_1 silencing (*siCB_1*) on melanin content and CB_1 mRNA and protein expression (*inset*). *D*, effect of mAEA (1 μM) alone or in combination with SB203580 (10 μM) or PD98059 (10 μM) on melanin synthesis. In *B*, SR141716, SR144528, and I-RTX were ineffective when used alone (not shown for the sake of clarity). *Error bars* represent S.E. values. ***, $p < 0.001$ *versus* control (*Ctrl*). ###, $p < 0.001$ *versus* mAEA.

nificantly) additive (Fig. 6*C* and data not shown), suggesting that both substances increased melanogenesis through a somewhat overlapping signaling pathway. Remarkably, AEA did not significantly affect cAMP content in NHEM cells at variance with α-MSH and forskolin (used as a positive control) that increased it by ~2-fold over controls (Table 3). However, AEA increased pCREB content by ~2-fold over controls in a manner that depended on CB_1 and p38 and p42/44 MAPK activities (Table 4). Incidentally, the modest effect of AEA on intracellular cAMP content (58) and the ability of CB_1 to trigger CREB phosphorylation (59, 60) are not unprecedented. Additionally, the effect of AEA on pCREB levels was independent of PKA as suggested by the lack of effect of the PKA inhibitor H89; however, H89 fully blocked the increase of pCREB induced by α-MSH (Table 4) as expected (42).

DISCUSSION

In this study, we demonstrated the presence of a complete and fully functional ECS in primary human melanocytes. These cells were chosen because they are a truly physiological model devoid of the genetic alterations possibly present in the easier-to-grow immortalized melanoma cells (61). In addition, we discovered that non-cytotoxic doses of eCBs can enhance melanin synthesis through a CB_1-dependent activation of tyrosinase gene expression mediated by p38 and p42/44 MAPKs, CREB, and the regulator MITF. Higher concentrations of eCBs trigger programmed death of NHEM cells via a TRPV1-dependent mechanism that involves p53. These findings are summarized in Fig. 7*A*.

The presence of a fully functional ECS in NHEM cells suggested that eCBs could play a role in controlling the cell choice between growth and death, a rather common effect of these endogenous compounds in different cell types (46, 62, 63), including keratinocytes (19, 64). We found that indeed mAEA dose-dependently reduced NHEM cell viability at concentrations of 5 μM or more (Fig. 2*A*) due to induction of apoptosis (Fig. 2*B*). This effect of mAEA was replicated by natural agonists of TRPV1 receptors such as AEA and CPS and was prevented by a selective antagonist of this receptor such as I-RTX (Fig. 2*C*); thus, also in NHEM cells, the death program involved TRPV1 as already found in many other cell types (46).

However, the most interesting observation of this investigation is that mAEA and other natural eCBs (AEA and 2-AG) that bind to and activate CB_1 receptors are able to enhance melanin synthesis at a dose of 1 μM (Fig. 3, *A* and *B*). CB_1 binding triggers p38 and p42/44 MAPK activities (Fig. 3*C*), two signaling pathways commonly engaged by this receptor subtype (35, 65, 66), and hence it phosphorylates CREB, which is a recently discovered target of CB_1 (59, 60). In turn, pCREB enhances tyrosinase gene expression and activity (Fig. 4) through the enhancement of the upstream regulator MITF (Fig. 5). A similar p38 and p42/44 MAPK-dependent activation of melanin synthesis through tyrosinase up-regulation was also induced by α-MSH through MC1R receptor (Fig. 6, *A* and *B*). However, a major

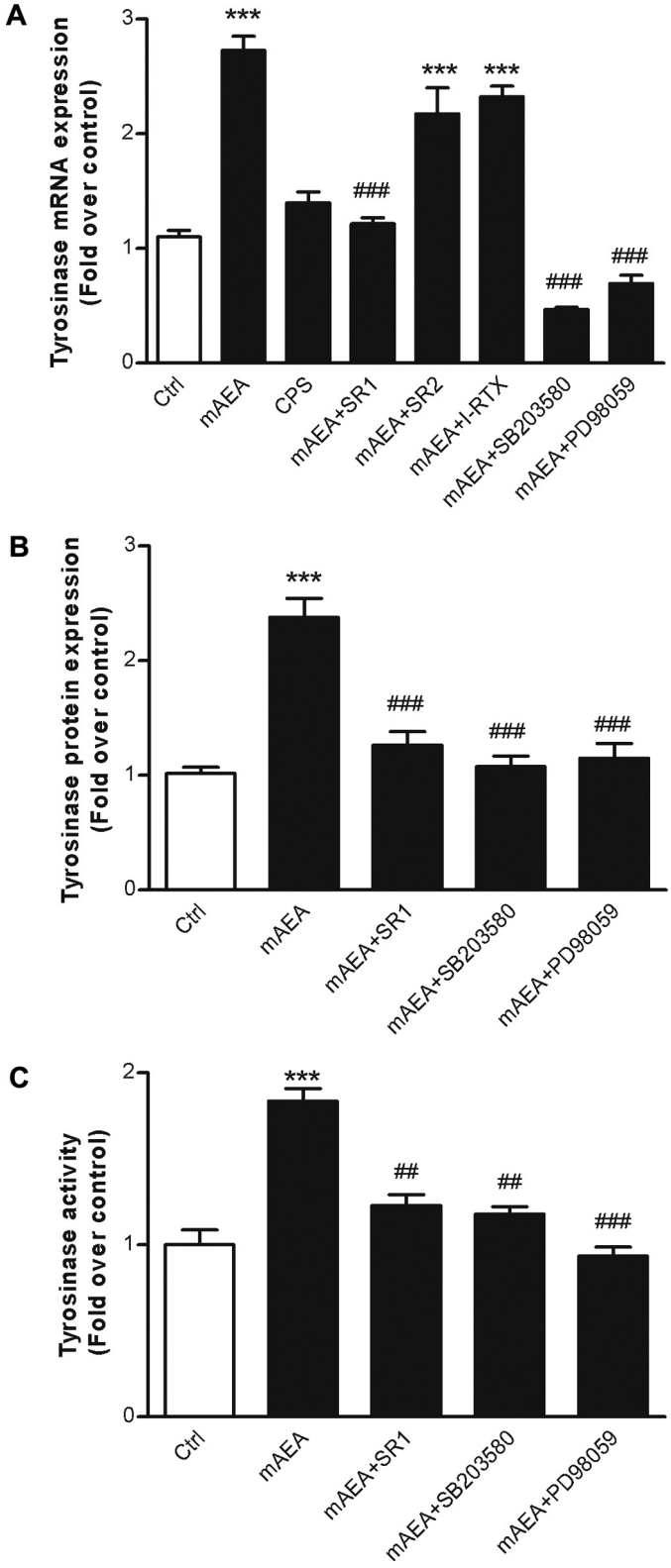

FIGURE 4. **Induction of tyrosinase expression and activity by mAEA and related compounds.** *A*, induction of tyrosinase mRNA levels by mAEA or CPS (each used at 1 μM) and of mAEA (1 μM) in combination with SR141716 (*SR1*; 0.1 μM), SR144528 (*SR2*; 0.1 μM), I-RTX (1 μM), SB203580 (10 μM), or PD98059 (10 μM). Induction of tyrosinase protein expression (*B*) and of tyrosinase activity (*C*) by mAEA (1 μM) alone or in combination with SR141716 (*SR1*), SB203580, or PD98059 as detailed in *A*. In all panels, SR141716, SR144528, I-RTX, SB203580, and PD98059 were ineffective when used alone (not shown for the sake of clarity). *Error bars* represent S.E. ***, $p < 0.001$ *versus* control (*Ctrl*). ##, $p < 0.05$; ###, $p < 0.001$ *versus* mAEA.

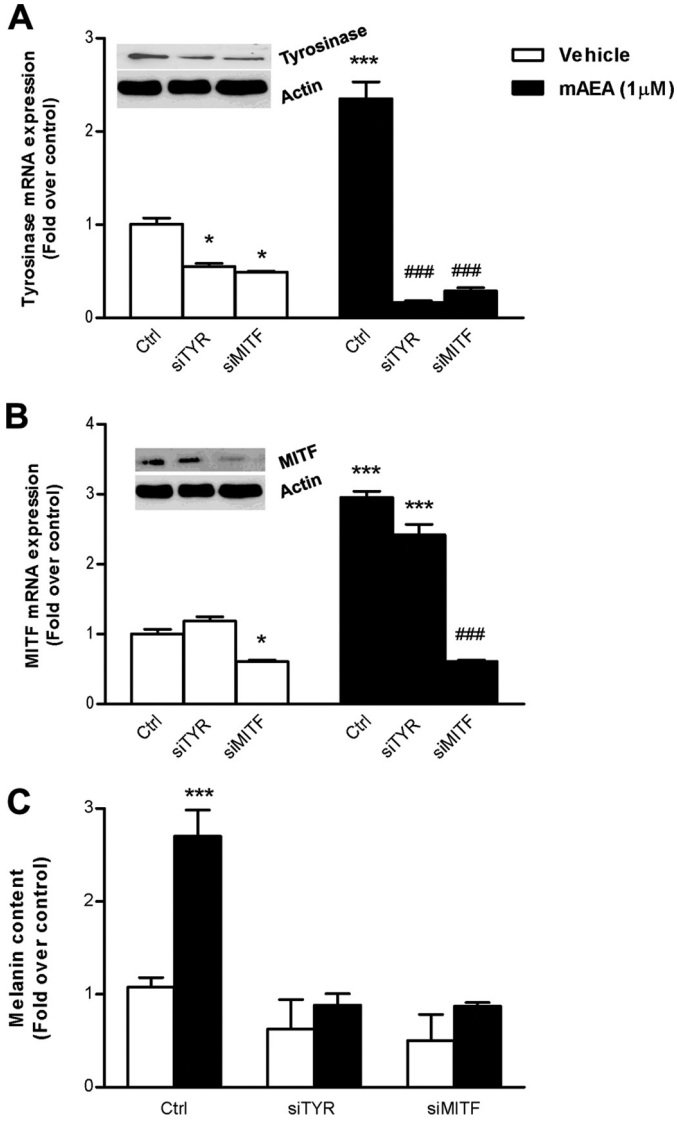

FIGURE 5. **Effect of tyrosinase and MITF silencing on mAEA activity.** *A*, RNA interference of tyrosinase (*siTYR*) or MITF (*siMITF*) reduced tyrosinase mRNA and abrogated the ability of mAEA to induce its expression. *B*, RNA interference of tyrosinase (*siTYR*) did not reduce MITF mRNA nor did it abrogate the ability of mAEA to induce its expression. However, RNA interference of MITF (*siMITF*) had both effects. *C*, RNA interference of tyrosinase (*siTYR*) or MITF (*siMITF*) abrogated the ability of mAEA to induce melanin synthesis. *Error bars* represent S.E. values. *, $p < 0.05$; ***, $p < 0.001$ *versus* control (*Ctrl*). ###, $p < 0.001$ *versus* controls treated with 1 μM mAEA.

difference between AEA and α-MSH is that the former does not affect cAMP content, which however is increased by the latter compound (Table 3). In this context, it seems interesting to note that a recent report has elucidated a novel pathway that regulates melanogenesis via the CREB-specific coactivator 1 (TORC1) in murine melanoma cells without affecting cAMP levels (67). In general, it seems noteworthy that melanogenesis induced by eCBs could represent a much faster alternative to the α-MSH-dependent pathway. In fact, the latter can activate MITF (and hence tyrosinase) only after enhancing the proopiomelanocortin gene expression and the cleavage of its protein product into γ-MSH, adrenocorticotrophic hormone (ACTH), and β-lipotropic hormone and finally the conversion of ACTH into α-MSH (31). However, eCBs such as AEA or 2-AG can be

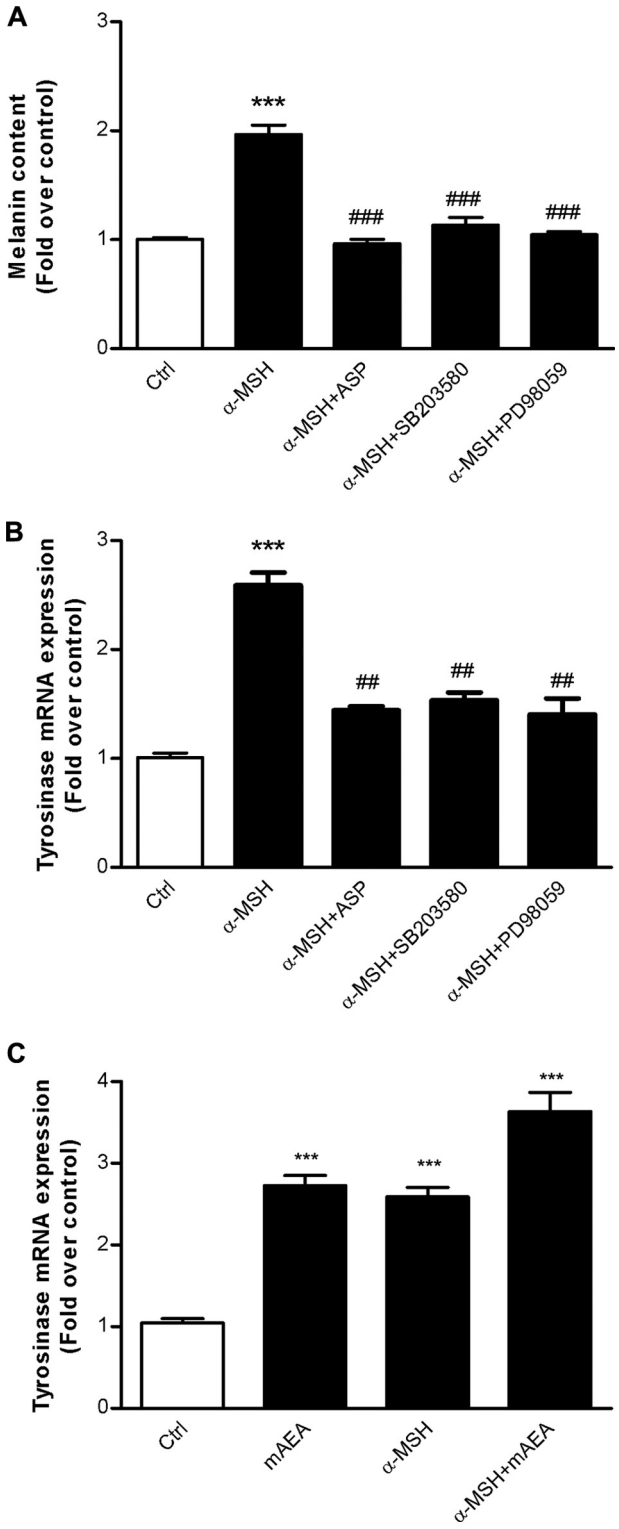

FIGURE 6. **Induction of melanogenesis by α-MSH.** The effect of α-MSH (100 nM) alone or in combination with Agouti-related signaling protein (*ASP*; 10 nM), SB203580 (10 μM), and PD98059 (10 μM) on melanin content (*A*) and tyrosinase mRNA expression (*B*) is shown. *C*, effect of mAEA (1 μM), α-MSH (100 nM), and their combination on tyrosinase mRNA. *Error bars* represent S.E. values. ***, $p < 0.001$ *versus* control (*Ctrl*). ##, $p < 0.05$; ###, $p < 0.001$ *versus* α-MSH.

released very rapidly from cell membranes through the hydrolysis of phospholipid precursors catalyzed by specific enzymes already present in the cell (for a review, see Ref. 9). This hypothesis is schematically represented in Fig. 7*B*. It can also be speculated that keratinocytes surrounding melanocytes in a ~35:1 ratio (29) can be a source of AEA. In fact, when we compared the amount of AEA (pmol/mg of protein) with the number of cells needed to yield 1 mg of protein using human keratinocytes of a known diameter and a purported spherical shape such as immortalized HaCaT cells (diameter, 28 μm; 2×10^6 cells/mg of protein) or primary normal human epidermal keratinocyte cells (diameter 22 μm; 4×10^6 cells/mg of protein) from previous data (19), we could estimate that the intracellular concentration of AEA in human keratinocytes is ~2 μM. This amount is in the concentration range needed to induce melanogenesis (Fig. 3*A*), thus adding physiological meaning to the present findings. Furthermore, it has been demonstrated that mouse epidermal cells (68) and human HaCaT cells (69) can synthesize AEA in response to ultraviolet B irradiation, a typical stimulus for melanogenesis (30). The level of 2-AG and the 2-AG/AEA ratio is increased in irradiated HaCaT cells (69), suggesting that UV light or other stress conditions may lead keratinocytes to release CB_1-binding eCBs, thus triggering melanin synthesis in the nearby melanocytes as a protective response for the keratinocytes themselves. Seemingly contradictory data were reported in a study published during the preparation of this manuscript. It showed that the synthetic CB_1 agonist ACEA did not affect melanin production by a human melanoma cell line (SK-mel-1) in monoculture, yet it reduced basal melanogenesis when SK-mel-1 were co-cultured with HaCaT cells (69). However, it is important to note that the molecular details at the basis of the loss of responsiveness of immortalized melanoma cells to CB_1-binding eCBs remain elusive even though an altered expression of MITF in these cells compared with primary melanocytes could be envisaged (61). On the other hand, the study by Magina *et al.* (69) suggests that keratinocytes respond to ACEA by releasing an inhibitor of melanogenesis, but the identity of this inhibitor is unknown, and no informa-

TABLE 3
Content of cAMP in human NHEM cells treated with mAEA, α-MSH, or forskolin

NHEM treatment	cAMP concentration (μM)
Ctrl	3.45 ± 0.49
mAEA (1 μM)	4.57 ± 0.52
α-MSH (100 nM)	8.50 ± 1.20[a]
Forskolin (20 μM)	9.55 ± 1.90[a]

[a] $p < 0.05$ *versus* control (Ctrl).

TABLE 4
Levels of pCREB in human NHEM cells treated with mAEA, α-MSH, and related compounds

SR141716, SB203580, PD98059, and H89 were ineffective when used alone under the same experimental conditions (omitted for the sake of clarity).

NHEM treatment	pCREB level ($A_{450\ nm}$)
Ctrl	0.347 ± 0.034
mAEA (1 μM)	0.749 ± 0.055[a]
mAEA (1 μM) + SR141716 (0.1 μM)	0.415 ± 0.092[b]
mAEA (1 μM) + SB203580 (10 μM)	0.476 ± 0.063[c]
mAEA (1 μM) + PD98059 (10 μM)	0.409 ± 0.015[b]
mAEA (1 μM) + H89 (5 μM)	0.691 ± 0.079[a]
α-MSH (100 nM)	0.702 ± 0.111[a]
α-MSH (100 nM) + H89 (5 μM)	0.383 ± 0.035[d]

[a] $p < 0.01$ *versus* control (Ctrl).
[b] $p < 0.01$ *versus* mAEA.
[c] $p < 0.05$ *versus* mAEA.
[d] $p < 0.05$ *versus* α-MSH.

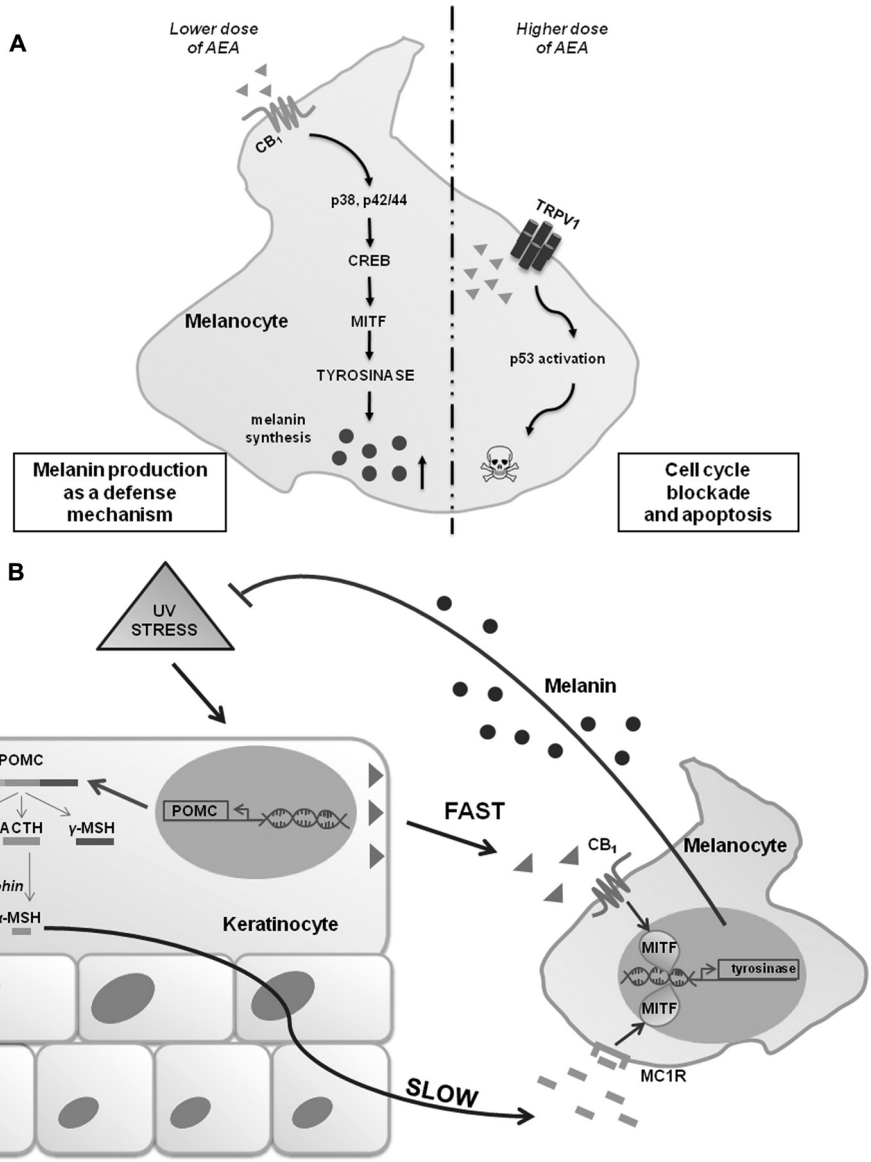

FIGURE 7. **Overall scheme of hypothetical effect of endocannabinoid signaling in human melanocytes.** *A*, low doses of AEA (~1 μM) and other CB_1-binding endocannabinoids stimulate melanogenesis through a p38- and p42/44-mediated pathway, which activates CREB and hence tyrosinase expression through the master regulator MITF. However, at higher doses (~5 μM or above), AEA promotes programmed cell death through a TRPV1-dependent pathway that engages p53. *B*, stimulation of melanogenesis by endocannabinoids (*triangles*) via CB_1 receptors can be a faster alternative compared with the classical route activated by α-MSH. In fact, the latter pathway requires proopiomelanocortin (*POMC*) expression and cleavage into an ACTH intermediate, which then matures into the final signaling molecule, α-MSH. Both routes might be triggered in keratinocytes by UV light or other stress factors to stimulate production by melanocytes of the protective agent melanin. *β-LPH*, β-lipotropic hormone.

tion about the signaling responsible for the HaCaT-SK-mel-1 cell cross-talk was available. In addition, it is also possible that the known ability of CB_1 receptors to antagonize the elevation of cAMP induced by several activators (58) might play a role in reducing basal melanogenesis in HaCaT-SK-mel-1 cell cocultures. Finally, it should be recalled that an increased eCB content has been previously reported in mouse skin upon acute and chronic contact dermatitis (70), in macrophages treated with lipopolysaccharide (71), and in neurons exposed to excitotoxic insults (72).

Altogether, eCBs seem to have a double effect on human melanocytes: (i) to induce melanogenesis at low concentrations through CB_1 receptors and (ii) to induce apoptosis at high concentrations through TRPV1 receptors. Incidentally, the need for higher concentrations of ligand to activate TRPV1 compared with those needed to activate CB_1 is consistent with the lower affinity of AEA (and of its stable analog mAEA) for TRPV1 in comparison with CB_1 as clearly demonstrated *in vitro* through binding assays (3). Both activities of eCBs might open the way to the development of ECS-targeted drugs as new tools to control melanogenesis in humans (by acting through CB_1) or to stop melanocyte proliferation and hence melanoma growth (by acting through TRPV1). It should be noted that the prevalence of skin cancer of which melanoma is perhaps the most severe form and the most metastasizing is growing faster than all other types of cancer (73). The presence of ECS in NHEM cells found at the mRNA, protein, and functional levels (Fig. 1 and Table 1) and already demonstrated in human kera-

tinocytes (19), hair follicles (20), and sebocytes (23) clearly supports a key role of eCB signaling within the skin. This hypothesis is also strengthened by the manifold effects shown by ECS modulation in this organ (for reviews, see Refs. 14 and 15). This may possibly lead to the therapeutic exploitation of ECS-targeted drugs to treat itch (17), allergic contact dermatitis (24), premature hair follicle regression (catagen) (20), allergic and chronic skin diseases (74), and other skin disorders characterized by sebaceous gland dysfunctions (*e.g.* acne vulgaris, seborrhea, and dry skin) (23). As a further remark, it is noteworthy that MITF plays other major roles outside skin, for instance in retinal pigmented epithelium, osteoclast development, mast cell functions, and clear cell sarcoma growth (31, 47). Therefore, our findings that identify eCBs as novel modulators of MITF might be relevant well beyond skin biology. It is also worth mentioning that eCBs have been shown to act as intercellular messengers in platelet-immune cell (68), neuron-astrocyte (75), and oocyte-sperm (36) communication. Thus, melanocyte-keratinocyte appears to be a new pair in this ever growing list.

Acknowledgment—We thank Dr. Giuseppina Catanzaro (University of Teramo) for kind assistance with preliminary biochemical assays of ECS elements in NHEM cells.

REFERENCES

1. Hanus, L. O., and Mechoulam, R. (2010) Novel natural and synthetic ligands of the endocannabinoid system. *Curr. Med. Chem.* **17,** 1341–1359
2. Howlett, A. C., Blume, L. C., and Dalton, G. D. (2010) CB_1 cannabinoid receptors and their associated proteins. *Curr. Med. Chem.* **17,** 1382–1393
3. Pertwee, R. G. (2010) Receptors and channels targeted by synthetic cannabinoid receptor agonists and antagonists. *Curr. Med. Chem.* **17,** 1360–1381
4. Di Marzo, V., and De Petrocellis, L. (2010) Endocannabinoids as regulators of transient receptor potential (TRP) channels: a further opportunity to develop new endocannabinoid-based therapeutic drugs. *Curr. Med. Chem.* **17,** 1430–1449
5. Okamoto, Y., Tsuboi, K., and Ueda, N. (2009) Enzymatic formation of anandamide. *Vitam. Horm.* **81,** 1–24
6. Petrosino, S., Ligresti, A., and Di Marzo, V. (2009) Endocannabinoid chemical biology: a tool for the development of novel therapies. *Curr. Opin. Chem. Biol.* **13,** 309–320
7. McKinney, M. K., and Cravatt, B. F. (2005) Structure and function of fatty acid amide hydrolase. *Annu. Rev. Biochem.* **74,** 411–432
8. Di Marzo, V. (2008) Endocannabinoids: synthesis and degradation. *Rev. Physiol. Biochem. Pharmacol.* **160,** 1–24
9. Maccarrone, M., Dainese, E., and Oddi, S. (2010) Intracellular trafficking of anandamide: new concepts for signaling. *Trends Biochem. Sci.* **35,** 601–608
10. Simon, G. M., and Cravatt, B. F. (2010) Activity-based proteomics of enzyme superfamilies: serine hydrolases as a case study. *J. Biol. Chem.* **285,** 11051–11055
11. Ross, R. A. (2009) The enigmatic pharmacology of GPR55. *Trends Pharmacol. Sci.* **30,** 156–163
12. Pistis, M., and Melis, M. (2010) From surface to nuclear receptors: the endocannabinoid family extends its assets. *Curr. Med. Chem.* **17,** 1450–1467
13. Ligresti, A., Petrosino, S., and Di Marzo, V. (2009) From endocannabinoid profiling to 'endocannabinoid therapeutics'. *Curr. Opin. Chem. Biol.* **13,** 321–331
14. Bíró, T., Tóth, B. I., Haskó, G., Paus, R., and Pacher, P. (2009) The endocannabinoid system of the skin in health and disease: novel perspectives and therapeutic opportunities. *Trends Pharmacol. Sci.* **30,** 411–420
15. Pasquariello, N., Oddi, S., Malaponti, M., and Maccarrone, M. (2009) Regulation of gene transcription and keratinocyte differentiation by anandamide. *Vitam. Horm.* **81,** 441–467
16. Pucci, M., Pirazzi, V., Pasquariello, N., and Maccarrone, M. (2011) Endocannabinoid signaling and epidermal differentiation. *Eur. J. Dermatol.* **21,** 29–34
17. Paus, R., Schmelz, M., Bíró, T., and Steinhoff, M. (2006) Frontiers in pruritus research: scratching the brain for more effective itch therapy. *J. Clin. Investig.* **116,** 1174–1186
18. Kupczyk, P., Reich, A., and Szepietowski, J. C. (2009) Cannabinoid system in the skin—a possible target for future therapies in dermatology. *Exp. Dermatol.* **18,** 669–679
19. Maccarrone, M., Di Rienzo, M., Battista, N., Gasperi, V., Guerrieri, P., Rossi, A., and Finazzi-Agrò, A. (2003) The endocannabinoid system in human keratinocytes. Evidence that anandamide inhibits epidermal differentiation through CB1 receptor-dependent inhibition of protein kinase C, activation protein-1, and transglutaminase. *J. Biol. Chem.* **278,** 33896–33903
20. Telek, A., Bíró, T., Bodó, E., Tóth, B. I., Borbíró, I., Kunos, G., and Paus, R. (2007) Inhibition of human hair follicle growth by endo- and exocannabinoids. *FASEB J.* **21,** 3534–3541
21. Ibrahim, M. M., Porreca, F., Lai, J., Albrecht, P. J., Rice, F. L., Khodorova, A., Davar, G., Makriyannis, A., Vanderah, T. W., Mata, H. P., and Malan T. P. (2005) CB2 cannabinoid receptor activation produces antinociception by stimulating peripheral release of endogenous opioids. *Proc. Natl. Acad. Sci. U.S.A.* **102,** 3093–3098
22. Khasabova, I. A., Khasabov, S. G., Harding-Rose, C., Coicou, L. G., Seybold, B. A., Lindberg, A. E., Steevens, C. D., Simone, D. A., and Seybold, V. S. (2008) A decrease in anandamide signaling contributes to the maintenance of cutaneous mechanical hyperalgesia in a model of bone cancer pain. *J. Neurosci.* **28,** 11141–11152
23. Dobrosi, N., Tóth, B. I., Nagy, G., Dózsa, A., Géczy, T., Nagy, L., Zouboulis, C. C., Paus, R., Kovács, L., and Bíró, T. (2008) Endocannabinoids enhance lipid synthesis and apoptosis of human sebocytes via cannabinoid receptor-2-mediated signaling. *FASEB J.* **22,** 3685–3695
24. Karsak, M., Gaffal, E., Date, R., Wang-Eckhardt, L., Rehnelt, J., Petrosino, S., Starowicz, K., Steuder, R., Schlicker, E., Cravatt, B., Mechoulam, R., Buettner, R., Werner, S., Di Marzo, V., Tüting, T., and Zimmer, A. (2007) Attenuation of allergic contact dermatitis through the endocannabinoid system. *Science* **316,** 1494–1497
25. Blázquez, C., Carracedo, A., Barrado, L., Real, P. J., Fernández-Luna, J. L., Velasco, G., Malumbres, M., and Guzmán, M. (2006) Cannabinoid receptors as novel targets for the treatment of melanoma. *FASEB J.* **20,** 2633–2635
26. Scuderi, M. R., Cantarella, G., Scollo, M., Lempereur, L., Palumbo, M., Saccani-Jotti, G., and Bernardini, R. (2011) The antimitogenic effect of the cannabinoid receptor agonist WIN55212-2 on human melanoma cells is mediated by the membrane lipid raft. *Cancer Lett.* **310,** 240–249
27. Choi, T. Y., Park, S. Y., Jo, J. Y., Kang, G., Park, J. B., Kim, J. G., Hong, S. G., Kim, C. D., Lee, J. H., and Yoon, T. J. (2009) Endogenous expression of TRPV1 channel in cultured human melanocytes. *J. Dermatol. Sci.* **56,** 128–130
28. Bronner-Fraser, M., and Fraser, S. E. (1988) Cell lineage analysis reveals multipotency of some avian neural crest cells. *Nature* **335,** 161–164
29. Smit, N., Vicanova, J., and Pavel, S. (2009) The hunt for natural skin whitening agents. *Int. J. Mol. Sci.* **10,** 5326–5349
30. Abdel-Malek, Z. A., Kadekaro A. L., and Swope, V. B. (2010) Stepping up melanocytes to the challenge of UV exposure. *Pigment Cell Melanoma Res.* **23,** 171–186
31. Liu, J. J., and Fisher, D. E. (2010) Lighting a path to pigmentation: mechanisms of MITF induction by UV. *Pigment Cell Melanoma Res.* **23,** 741–745
32. Simon, J. D., Peles, D., Wakamatsu, K., and Ito, S. (2009) Current challenges in understanding melanogenesis: bridging chemistry, biological control, morphology, and function. *Pigment Cell Melanoma Res.* **22,** 563–579
33. Johnson, S. L., Nguyen, A. N., and Lister, J. A. (2011) mitfa is required at multiple stages of melanocyte differentiation but not to establish the mel-

anocyte stem cell. *Dev. Biol.* **350,** 405–413
34. Bari, M., Battista, N., Fezza, F., Finazzi-Agrò, A., and Maccarrone, M. (2005) Lipid rafts control signaling of type-1 cannabinoid receptors in neuronal cells. Implications for anandamide-induced apoptosis. *J. Biol. Chem.* **280,** 12212–12220
35. Pasquariello, N., Catanzaro, G., Marzano, V., Amadio, D., Barcaroli, D., Oddi, S., Federici, G., Urbani, A., Finazzi Agrò, A., and Maccarrone, M. (2009) Characterization of the endocannabinoid system in human neuronal cells and proteomic analysis of anandamide-induced apoptosis. *J. Biol. Chem.* **284,** 29413–29426
36. Francavilla, F., Battista, N., Barbonetti, A., Vassallo, M. R., Rapino, C., Antonangelo, C., Pasquariello, N., Catanzaro, G., Barboni, B., and Maccarrone, M. (2009) Characterization of the endocannabinoid system in human spermatozoa and involvement of transient receptor potential vanilloid 1 receptor in their fertilizing ability. *Endocrinology* **150,** 4692–4700
37. Fezza, F., Gasperi, V., Mazzei, C., and Maccarrone, M. (2005) Radiochromatographic assay of *N*-acyl-phosphatidylethanolamine-specific phospholipase D activity. *Anal. Biochem.* **339,** 113–120
38. Gattinoni, S., De Simone, C., Dallavalle, S., Fezza, F., Nannei, R., Battista, N., Minetti, P., Quattrociocchi, G., Caprioli, A., Borsini, F., Cabri, W., Penco, S., Merlini, L., and Maccarrone, M. (2010) A new group of oxime carbamates as reversible inhibitors of fatty acid amide hydrolase. *Bioorg. Med. Chem. Lett.* **20,** 4406–4411
39. Bisogno, T., Howell, F., Williams, G., Minassi, A., Cascio, M. G., Ligresti, A., Matias, I., Schiano-Moriello, A., Paul, P., Williams, E. J., Gangadharan, U., Hobbs, C., Di Marzo, V., and Doherty, P. (2003) Cloning of the first sn1-DAG lipases points to the spatial and temporal regulation of endocannabinoid signaling in the brain. *J. Cell Biol.* **163,** 463–468
40. Dinh, T. P., Carpenter, D., Leslie, F. M., Freund, T. F., Katona, I., Sensi, S. L., Kathuria, S., and Piomelli, D. (2002) Brain monoglyceride lipase participating in endocannabinoid inactivation. *Proc. Natl. Acad. Sci. U.S.A.* **99,** 10819–10824
41. Xiao, L., Matsubayashi, K., and Miwa, N. (2007) Inhibitory effect of the water-soluble polymer-wrapped derivative of fullerene on UVA-induced melanogenesis via downregulation of tyrosinase expression in human melanocytes and skin tissues. *Arch. Dermatol. Res.* **299,** 245–257
42. Cheli, Y., Luciani, F., Khaled, M., Beuret, L., Bille, K., Gounon, P., Ortonne, J. P., Bertolotto, C., and Ballotti, R. (2009) αMSH and cyclic AMP elevating agents control melanosome pH through a protein kinase A-independent mechanism. *J. Biol. Chem.* **284,** 18699–18706
43. Werz, O., Klemm, J., Samuelsson, B., and Rådmark, O. (2001) Phorbol ester up-regulates capacities for nuclear translocation and phosphorylation of 5-lipoxygenase in Mono Mac 6 cells and human polymorphonuclear leukocytes. *Blood* **97,** 2487–2495
44. Colombo, G., Rusconi, F., Rubino, T., Cattaneo, A., Martegani, E., Parolaro, D., Bachi, A., and Zippel, R. (2009) Transcriptomic and proteomic analyses of mouse cerebellum reveals alterations in RasGRF1 expression following *in vivo* chronic treatment with Δ9-tetrahydrocannabinol. *J. Mol. Neurosci.* **37,** 111–122
45. Siegmund, S. V., Seki, E., Osawa, Y., Uchinami, H., Cravatt, B. F., and Schwabe, R. F. (2006) Fatty acid amide hydrolase determines anandamide-induced cell death in the liver. *J. Biol. Chem.* **281,** 10431–10438
46. Maccarrone, M. (2006) in *Endocannabinoids: the Brain and Body's Marijuana and Beyond* (Onaivi, E. S., Sugiura, T., and Di Marzo, V., eds) pp. 451–466, CRC Press, Boca Raton, FL
47. Cheli, Y., Ohanna, M., Ballotti, R., and Bertolotto, C. (2010) Fifteen-year quest for microphthalmia-associated transcription factor target genes. *Pigment Cell Melanoma Res.* **23,** 27–40
48. Buscà, R., and Ballotti, R. (2000) Cyclic AMP a key messenger in the regulation of skin pigmentation. *Pigment Cell Res.* **13,** 60–69
49. Wan, P., Hu, Y., and He, L. (2011) Regulation of melanocyte pivotal transcription factor MITF by some other transcription factors. *Mol. Cell. Biochem.* **354,** 241–246
50. Tada, A., Pereira, E., Beitner-Johnson, D., Kavanagh, R., and Abdel-Malek, Z. A. (2002) Mitogen- and ultraviolet-B-induced signaling pathways in normal human melanocytes. *J. Invest. Dermatol.* **118,** 316–322
51. Shaywitz, A. J., and Greenberg, M. E. (1999) CREB: a stimulus-induced transcription factor activated by a diverse array of extracellular signals. *Annu. Rev. Biochem.* **68,** 821–861
52. Buscà, R., Abbe, P., Mantoux, F., Aberdam, E., Peyssonnaux, C., Eychène, A., Ortonne, J. P., and Ballotti, R. (2000) Ras mediates the cAMP-dependent activation of extracellular signal-regulated kinases (ERKs) in melanocytes. *EMBO J.* **19,** 2900–2910
53. Hemesath, T. J., Price, E. R., Takemoto, C., Badalian, T., and Fisher, D. E. (1998) MAP kinase links the transcription factor microphthalmia to c-Kit signalling in melanocytes. *Nature* **391,** 298–301
54. Price, E. R., Ding, H. F., Badalian, T., Bhattacharya, S., Takemoto, C., Yao, T. P., Hemesath, T. J., and Fisher, D. E. (1998) Lineage-specific signaling in melanocytes. c-kit stimulation recruits p300/CBP to microphthalmia. *J. Biol. Chem.* **273,** 17983–17986
55. Xu, W., Gong, L., Haddad, M. M., Bischof, O., Campisi, J., Yeh, E. T., and Medrano, E. E. (2000) Regulation of microphthalmia-associated transcription factor MITF protein levels by association with the ubiquitin-conjugating enzyme hUBC9. *Exp. Cell Res.* **255,** 135–143
56. Corre, S., Mekideche, K., Adamski, H., Mosser, J., Watier, E., and Galibert, M. D. (2006) *In vivo* and *ex vivo* UV-induced analysis of pigmentation gene expressions. *J. Invest. Dermatol.* **126,** 916–918
57. Park, S. Y., Kim, Y. H., Kim, Y. H., Park, G., and Lee, S. J. (2010) β-Carboline alkaloids harmaline and harmalol induce melanogenesis through p38 mitogen-activated protein kinase in B16F10 mouse melanoma cells. *BMB Rep.* **43,** 824–829
58. Felder, C. C., Briley, E. M., Axelrod, J., Simpson, J. T., Mackie, K., and Devane, W. A. (1993) Anandamide, an endogenous cannabimimetic eicosanoid, binds to the cloned human cannabinoid receptor and stimulates receptor-mediated signal transduction. *Proc. Natl. Acad. Sci. U.S.A.* **90,** 7656–7660
59. Casu, M. A., Pisu, C., Sanna, A., Tambaro, S., Spada, G. P., Mongeau, R., and Pani, L. (2005) Effect of Δ9-tetrahydrocannabinol on phosphorylated CREB in rat cerebellum: an immunohistochemical study. *Brain Res.* **1048,** 41–47
60. Zorina, Y., Iyengar, R., and Bromberg, K. D. (2010) Cannabinoid 1 receptor and interleukin-6 receptor together induce integration of protein kinase and transcription factor signaling to trigger neurite outgrowth. *J. Biol. Chem.* **285,** 1358–1370
61. Levy, C., Khaled, M., and Fisher, D. E. (2006) MITF: master regulator of melanocyte development and melanoma oncogene. *Trends Mol. Med.* **12,** 406–414
62. Bifulco, M., and Di Marzo, V. (2002) Targeting the endocannabinoid system in cancer therapy: a call for further research. *Nat. Med.* **8,** 547–550
63. Guzmán, M. (2003) Cannabinoids: potential anticancer agents. *Nat. Rev. Cancer* **3,** 745–755
64. Casanova, M. L., Blázquez, C., Martínez-Palacio, J., Villanueva, C., Fernández-Aceñero, M. J., Huffman, J. W., Jorcano, J. L., and Guzmán, M. (2003) Inhibition of skin tumor growth and angiogenesis in vivo by activation of cannabinoid receptors. *J. Clin. Investig.* **111,** 43–50
65. Bouaboula, M., Poinot-Chazel, C., Bourrié, B., Canat, X., Calandra, B., Rinaldi-Carmona, M., Le Fur, G., and Casellas, P. (1995) Activation of mitogen-activated protein kinases by stimulation of the central cannabinoid receptor CB1. *Biochem. J.* **312,** 637–641
66. Liu, J., Gao, B., Mirshahi, F., Sanyal, A. J., Khanolkar, A. D., Makriyannis, A., and Kunos, G. (2000) Functional CB1 cannabinoid receptors in human vascular endothelial cells. *Biochem. J.* **346,** 835–840
67. Kumagai, A., Horike, N., Satoh, Y., Uebi, T., Sasaki, T., Itoh, Y., Hirata, Y., Uchio-Yamada, K., Kitagawa, K., Uesato, S., Kawahara, H., Takemori, H., and Nagaoka, Y. (2011) A potent inhibitor of SIK2, 3,3′,7-trihydroxy-4′-methoxyflavon(4′-*O*-methylfisetin), promotes melanogenesis in B16F10 melanoma cells. *PLoS One* **6,** e26148
68. Berdyshev, E. V., Schmid, P. C., Krebsbach, R. J., and Schmid, H. H. (2001) Activation of PAF receptors results in enhanced synthesis of 2-arachidonoylglycerol (2-AG) in immune cells. *FASEB J.* **15,** 2171–2178
69. Magina, S., Esteves-Pinto, C., Moura, E., Serrão, M. P., Moura, D., Petrosino, S., Di Marzo, V., and Vieira-Coelho, M. A. (2011) Inhibition of basal and ultraviolet B-induced melanogenesis by cannabinoid CB_1 receptors: a keratinocyte-dependent effect. *Arch. Dermatol. Res.* **303,** 201–210
70. Oka, S., Wakui, J., Ikeda, S., Yanagimoto, S., Kishimoto, S., Gokoh, M.,

Nasui, M., and Sugiura, T. (2006) Involvement of the cannabinoid CB2 receptor and its endogenous ligand 2-arachidonoylglycerol in oxazolone-induced contact dermatitis in mice. *J. Immunol.* **177,** 8796–8805
71. Liu, J., Batkai, S., Pacher, P., Harvey-White, J., Wagner, J. A., Cravatt, B. F., Gao, B., and Kunos, G. (2003) Lipopolysaccharide induces anandamide synthesis in macrophages via CD14/MAPK/phosphoinositide 3-kinase/NF-κB independently of platelet-activating factor. *J. Biol. Chem.* **278,** 45034–45039
72. Marsicano, G., Goodenough, S., Monory, K., Hermann, H., Eder, M., Cannich, A., Azad, S. C., Cascio, M. G., Gutiérrez, S. O., van der Stelt, M., López-Rodriguez, M. L., Casanova, E., Schütz, G., Zieglgänsberger, W., Di Marzo, V., Behl, C., and Lutz, B. (2003) CB1 cannabinoid receptors and on-demand defense against excitotoxicity. *Science* **302,** 84–88
73. American Cancer Society (2009) *Cancer Facts & Figures 2009*, American Cancer Society, Atlanta
74. Sugawara, K., Bíró, T., Tsuruta, D., Tóth, B. I., Kromminga, A., Zákány, N., Zimmer, A., Funk, W., Gibbs, B. F., Zimmer, A., and Paus, R. (2012) Endocannabinoids limit excessive mast cell maturation and activation in human skin. *J. Allergy Clin. Immunol.* **129,** 726–738.e8
75. Navarrete, M., and Araque, A. (2008) Endocannabinoids mediate neuron-astrocyte communication. *Neuron* **57,** 883–893